ResearchGate

See discussions, stats, and author profiles for this publication at: https://www.researchgate.net/publication/253646186

Homo- and Heterometal Complexes of Oxido-Metal Ions with a Triangular [V(V)O-MO-V(V)O] [M = V(IV) and Re(V)] Core: Reporting Mixed-Oxidation Oxido-Vanadium(V/IV/V) Compounds with V...

ARTICLE *in* INORGANIC CHEMISTRY · JULY 2013

Impact Factor: 4.76 · DOI: 10.1021/ic4013203 · Source: PubMed

CITATIONS
6

READS
83

5 AUTHORS, INCLUDING:

Manoranjan Maity
Indian Institute of Science
10 PUBLICATIONS **82** CITATIONS
SEE PROFILE

Sk Md Towsif Abtab
King Abdullah University of Science and Techn...
15 PUBLICATIONS **143** CITATIONS
SEE PROFILE

Available from: Sk Md Towsif Abtab
Retrieved on: 02 February 2016

Inorganic Chemistry

Article

pubs.acs.org/IC

Homo- and Heterometal Complexes of Oxido−Metal Ions with a Triangular [V(V)O−MO−V(V)O] [M = V(IV) and Re(V)] Core: Reporting Mixed-Oxidation Oxido−Vanadium(V/IV/V) Compounds with Valence Trapped Structures

Kisholoy Bhattacharya, Manoranjan Maity, Sk Md Towsif Abtab, Mithun Chandra Majee, and Muktimoy Chaudhury*

Department of Inorganic Chemistry, Indian Association for the Cultivation of Science, Jadavpur, Kolkata 700 032, India

Supporting Information

ABSTRACT: A new family of trinuclear homo- and heterometal complexes with a triangular [V(V)O−MO−V(V)O] (M = V(IV), **1** and **2**; Re(V), **3**] all-oxido−metal core have been synthesized following a single-pot protocol using compartmental Schiff-base ligands, *N*,*N*′-bis(3-hydroxysalicylidene)-diiminoalkanes/arene (H_4L^1−H_4L^3). The upper compartment of these ligands with N_2O_2 donor combination (Salen-type) contains either a V(IV) or a Re(V) center, while the lower compartment with O_4 donor set accommodates two V(V) centers, stabilized by a terminal and a couple of bridging methoxido ligands. The compounds have been characterized by single-crystal X-ray diffraction analyses, which reveal octahedral geometry for all three metal centers in **1**−**3**. Compound **1** crystallizes in a monoclinic space group $P2_1/c$, while both **2** and **3** have more symmetric structures with orthorhombic space group *Pnma* that renders the vanadium(V) centers in these compounds exactly identical. In DMF solution, compound **1** displays an 8-line EPR at room temperature with ⟨*g*⟩ and ⟨*A*⟩ values of 1.972 and 86.61 × 10^{-4} cm^{-1}, respectively. High-resolution X-ray photoelectron spectrum (XPS) of this compound shows a couple of bands at 515.14 and 522.14 eV due to vanadium $2p_{3/2}$ and $2p_{1/2}$ electrons in the oxidation states +5 and +4, respectively. All of these, together with bond valence sum (BVS) calculation, confirm the trapped-valence nature of mixed-oxidation in compounds **1** and **2**. Electrochemically, compound **1** undergoes two one-electron oxidations at $E_{1/2}$ = 0.52 and 0.83 V vs Ag/AgCl reference. While the former is due to a metal-based V(IV/V) oxidation, the latter one at higher potential is most likely due to a ligand-based process involving one of the catecholate centers. A larger cavity size in the upper compartment of the ligand H_4L^3 is spacious enough to accommodate Re(V) with larger size to generate a rare type of all-oxido heterotrimetallic compound (**3**) as established by X-ray crystallography.

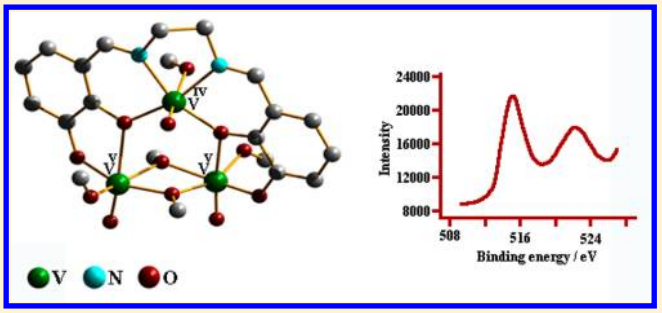

INTRODUCTION

Coordination chemistry of vanadium[1] deals with a large number of vanadium oxidation states ranging from −3 to +5. Among these, +4 and +5 are the most common oxidation states and can be accessed easily under aerobic conditions when the metal ion generates various types of oxido species. In these high oxidation states, vanadium shows distinct preference for N/O donor ligands in complex formation that leads to the development of a large part of its coordination chemistry, particularly in solution.[2] Out of the various types of oxido−vanadium compounds, mixed-oxidation (IV/V) complexes are of special interest because of their intriguing spectroscopic properties.[3] Among these, dinuclear mixed-valence oxido−vanadium complexes containing $[V_2O_3]^{3+}$ core are the most common in occurrence because of their favorable thermodynamic stability and ease of formation.[2c,d,4] Surprisingly, there are only a few reported examples of mixed-oxidation vanadium(IV/V) compounds with vanadium nuclearity higher than two.[4c,5]

Herein, we report two trinuclear mixed-oxidation vanadium(V/IV/V) complexes **1** and **2** together with a trinuclear heterometal complex **3** containing an oxido−rhenium(V) and a couple of oxido−vanadium(V) centers using hexadentate Schiff-base compartmental ligands having N_2O_4 donor combinations. The compounds have been characterized by single-crystal X-ray diffraction analyses, ESI−MS, EPR, and X-ray photoelectron spectroscopy. Bond valence sum (BVS) approach has been applied to confirm the oxidation states of the vanadium centers in **1** and **2**. Redox behavior of **1** has been investigated using the technique of cyclic voltammetry.

EXPERIMENTAL SECTION

Materials. The precursor complexes $[VO(acac)_2]$[6] and $[ReOCl_3(PPh_3)_2]$[7] were prepared following literature methods. 2,3-Dihydroxybenzaldehyde and 2,2-dimethyl-1,3-diaminopropane were

Received: May 27, 2013

 © XXXX American Chemical Society dx.doi.org/10.1021/ic4013203 | *Inorg. Chem.* XXXX, XXX, XXX−XXX

purchased from Aldrich. All other chemicals were commercially available and used as received. Solvents were reagent grade, dried by standard methods,[8] and distilled under nitrogen prior to their use.

Preparation of the Ligands. *N,N′-Bis(3-hydroxysalicylidene)-1,2-diaminoethane (H_4L^1).* To a stirred solution of 2,3-dihydroxybenzaldehyde (2.76 g, 20 mmol) in methanol (30 mL) was added ethylenediamine (0.6 g, 10 mmol), and the solution was refluxed for 30 min. It was cooled to room temperature and filtered to obtain an orange crystalline product. Yield: 2.2 g (73%). mp 170 °C. Anal. Calcd for $C_{17}H_{20}N_2O_5$: C, 61.44; H, 6.07; N, 8.43. Found: C, 61.69; H, 6.06; N, 8.15. ^{1}H NMR (400 MHz, DMSO-d_6, 298 K, δ/ppm): 13.88 (br s, 2H, phenolic−OH), 8.98 (br s, 2H, phenolic−OH), 8.48 (s, 2H, azomethine), 6.85 (m, 4H, phenyl ring), 6.66 (t, J = 8.0 Hz, 2H, phenyl ring), 3.48 (s, 4H, CH_2), 0.99 (s, 3H CH_3).

N,N′-Bis(3-hydroxysalicylidene)-1,2-diaminobenzene (H_4L^2). This ligand was obtained following the same procedure as that for H_4L^1 using *o*-phenylenediamine (1.08 g, 10 mmol) as a replacement for ethylenediamine. The product was collected as a dark red crystalline solid. Yield: 74%. mp 192 °C. Anal. Calcd for $C_{20}H_{16}N_2O_4$: C, 68.96; H, 4.63; N, 8.04. Found: C, 68.68; H, 4.71; N, 8.06. ^{1}H NMR (500 MHz, $CDCl_3$, 298 K, δ/ppm): 13.59 (br s, 2H, phenolic OH), 8.63 (s, 2H, azomethine), 7.31 (m, 4H phenyl ring), 7.02 (m, 4H, phenyl ring), 6.83 (m, 2H, phenyl ring), 6.04 (br s, 2H, phenolic OH). UV−vis (CH_2Cl_2) [λ_{max}, nm (ε, L mol^{-1} cm^{-1})]: 226 (18 300), 281 (18 100), 333 (13 900).

N,N′-Bis(3-hydroxysalicylidene)-2,2-dimethyl-1,3-diaminopropane (H_4L^3). This compound was synthesized following essentially the same procedure as that for H_4L^1 using 2,2-dimethyl-1,3-diaminopropane (1.02 g, 10 mmol) instead of ethylenediamine. The product was collected as an orange crystalline solid. Yield: 79%. mp 169 °C. Anal. Calcd for $C_{19}H_{22}N_2O_4$: C, 66.65; H, 6.48; N, 8.18. Found: C, 66.50; H, 6.50; N, 8.20. ^{1}H NMR (500 MHz, $CDCl_3$, 298 K, δ/ppm): 8.24 (s, 2H, azomethine), 6.97 (d, J = 8.0 Hz, 2H, phenyl ring), 6.79 (d, J = 8.0 Hz, 2H, phenyl ring), 6.70 (t, 2H, phenyl ring), 3.51 (s, 4H, methylene), 1.12 (s, 6H, methyl). UV−vis (CH_2Cl_2) [λ_{max}, nm (ε, L mol^{-1} cm^{-1})]: 225 (20 600), 263 (23 700), 302 (9800), 433 (2500).

Preparation of Complexes. *$[L^1\{(V^{IV}O)CH_3OH\}\{(V^{V}O)(OCH_3)(\mu\text{-}OCH_3)\}_2]\cdot CH_3OH$* **1**. To a stirred solution of H_4L^1 (0.75 g, 0.25 mmol) in methanol (50 mL) was added $[VO(acac)_2]$ in solid (0.195 g, 0.75 mmol), and the mixture was refluxed for 2 h. The solution was filtered and kept overnight in the air to obtain dark blue crystals. The product was collected by filtration and washed with methanol. Some of these crystals were of diffraction grade and used directly for X-ray crystallographic analysis. Yield: 0.080 g (53%). Anal. Calcd for $C_{22}H_{32}N_2O_{13}V_3$: C, 38.54; H, 4.71; N, 4.08. Found: C, 38.86, H, 4.58, N, 4.14. FT-IR bands (KBr pellet, cm^{-1}): 1639 vs, 1589 m, 1544 m, 1440 s, 1398 m, 1331 m, 1265 s, 1221 m, 1041 s, 976 vs, 775 m, 742 m, 661 m, 605 m, 561 m. ESI−MS (positive) in CH_2Cl_2: m/z, 644 $[M - 2CH_3OH+Na]^+$.

$[L^2\{(V^{V}O)CH_3OH\}\{(V^{V}O)(OCH_3)(\mu\text{-}OCH_3)\}_2]$ **2**. This compound was obtained following the same procedure as that described for **1** using H_4L^2 as a replacement for H_4L^1 as ligand to obtain dark green needle-shaped crystals. Yield: 0.073 g (41%). Anal. Calcd for $C_{25}H_{28}N_2O_{12}V_3$: C, 42.81; H, 4.02, N, 3.99. Found: C, 42.67; H, 3.91; N, 4.03. FT-IR bands (KBr pellet, cm^{-1}): 1608 vs, 1579 s, 1531 s, 1446 m, 1382 m, 1332 m, 1265 m, 1199 s, 991 vs, 887 w, 787 s, 744 s, 650 m, 578 m, 544 m. ESI−MS (positive) in CH_2Cl_2: m/z, 692 $[M - CH_3OH+Na]^+$.

$[L^3\{(Re^{V}O)(OCH_3)\}\{(V^{V}O)(OCH_3)(\mu\text{-}OCH_3)\}_2]$ **3**. To a stirred solution of H_4L^3 (0.068 g, 0.2 mmol) in methanol were added Et_3N (0.4 g, 0.4 mmol) and $[ReOCl_3(PPh_3)_2]$ (0.166 g, 0.2 mmol), and the solution was refluxed for 1 h during which time the color of the solution turned to green. The solution was cooled to room temperature, and $[VO(acac)_2]$ (0.104 g, 0.4 mmol) was added in solid to the reaction mixture. The resulting solution was refluxed further for 2 h. The solution was cooled to room temperature, filtered, and kept overnight in the air to get dark brown crystals. The product was collected by filtration, washed with methanol, and dried over $CaCl_2$. Some of these crystals were of diffraction grade and used directly for X-ray crystallographic analysis. Yield: 0.096 g (51%). Anal. Calcd for $C_{24}H_{33}N_2O_{12}ReV_2$: C, 34.74; H, 3.98; N, 3.38. Found: C, 34.86; H, 3.82; N, 3.41. FT-IR bands (KBr pellet, cm^{-1}): 1641 vs, 1591 s, 1540 s, 1456 s, 1360 m, 1335 m, 1255 s, 1209 m, 945 s, 910 s, 760 m, 682 m, 575 m, 522 m.

Physical Measurements. Elemental analyses (for C, H, and N) were performed at IACS on a Perkin-Elmer model 2400 Series II CHN Analyzer. The ^{1}H NMR spectra were recorded on Bruker model Avance DPX-500 and Avance DPX-400 spectrometers using $SiMe_4$ as internal reference. IR spectra of the samples prepared as KBr pellets were recorded using a Shimadzu model 8400S FT-IR spectrometer. The electrospray ionization mass spectra (ESI−MS) in positive ion mode were measured on a Micromass QTOF model YA 263 mass spectrometer. For UV−visible spectra in solution, a Perkin-Elmer model Lambda 950 UV/vis/NIR spectrophotometer was employed. EPR spectra in DMF solution were recorded on a JEOL model JES-FA 300 X-band spectrometer, equipped with a standard low temperature (77 K) apparatus and data processing system ESPRIT 330. The spectra at room temperature were recorded in a flat cell. X-ray photoelectron spectroscopic (XPS) (Omicron) measurements were done using an Mg Kα radiation source under 15 kV voltage and 5 mA current conditions.

Cyclic voltammetry (CV) in DMF was recorded on a EG&G PARC electrochemical analysis system using a planar EG&G PARC G0229 glassy carbon milli electrode as the working electrode and a platinum wire as counter electrode. Ag/AgCl was used for reference and Fc/Fc$^+$ couple as the internal standard. Solutions were ∼1.0 mM in samples and contained 0.1 M TBAP as supporting electrolyte.

X-ray Crystallography. Diffraction quality crystals of **1** (flakes, blue, 0.16 × 0.10 × 0.07 mm^3), **2** (needle, green, 0.17 × 0.13 × 0.09 mm^3), and **3** (flakes, brown, 0.15 × 0.09 × 0.05 mm^3) were collected from their respective reaction pots. Crystals were mounted on glass fibers coated with perfluoropolyether oil before mounting. Intensity data for the compounds were measured employing a Bruker SMART APEX II CCD diffractometer equipped with Mo Kα radiation (λ = 0.71073 Å) source using the $\omega/2\theta$ scan technique at 150 K. No crystal decay was observed during the data collections. The intensity data were corrected for empirical absorptions. In all cases, absorption corrections based on multiscans using the SADABS software[9] were applied.

The structures were solved by direct methods[10] and refined on F^2 by a full-matrix least-squares procedure[10] based on all data minimizing $R = \sum||F_o| - |F_c||/\sum|F_o|$, $wR = [\sum[w(F_o^2 - F_c^2)^2]/\sum(F_o^2)^2]^{1/2}$, and $S = [\sum[w(F_o^2 - F_c^2)^2]/(n - p)]^{1/2}$. SHELXL-97 was used for both structure solutions and refinements.[11] A summary of relevant crystallographic data and final refinement details has been given in Table 1. All non hydrogen atoms were refined anisotropically. The hydrogen atoms were calculated and isotropically fixed in the final refinement [d(C−H) = 0.95 Å, with the isotropic thermal parameter of U_{iso}(H) = 1.2U_{iso}(C)]. The SMART and SAINT-plus software packages[12] were used for data collection and reduction, respectively. Crystallographic diagrams were drawn using the DIAMOND software package.[13]

RESULTS AND DISCUSSION

Syntheses. The compartmental Schiff-base ligands H_4L^1−H_4L^3 have been synthesized in high yields (ca. 75%) following a simple condensation reaction in methanol. These ligands have two compartments as depicted in Scheme 1. The one with N_2O_2 donor combination is referred to as the "upper compartment", while the other providing an O_4 donor set is cited as the "lower compartment" in the following part of this discussion. The trinuclear mixed-oxidation oxido−vanadium [V(V)−V(IV)−V(V)] complexes $[L^1\{(V^{IV}O)CH_3OH\}\{(V^{V}O)(OCH_3)(\mu\text{-}OCH_3)\}_2]\cdot CH_3OH$ **1** and $[L^2\{(V^{IV}O)CH_3OH\}\{(V^{V}O)(OCH_3)(\mu\text{-}OCH_3)\}_2]$ **2** are obtained in moderate yields (ca. 45%) by a metathetical reaction (Scheme 1) when stoichiometric amounts of the compartmental ligand H_4L^1 (H_4L^2 for **2**) and $[VO(acac)_2]$ (1:3 mol ratio) are refluxed in methanol under aerobic environment. The obligatory steps

dx.doi.org/10.1021/ic4013203 | Inorg. Chem. XXXX, XXX, XXX−XXX

Table 1. Summary of Relevant X-ray Crystallographic Data for Compounds 1−3

parameters	1	2	3
composition	$C_{22}H_{32}N_2O_{13}V_3$	$C_{25}H_{28}N_2O_{12}V_3$	$C_{24}H_{33}N_2O_{12}ReV_2$
formula wt	685.32	701.32	829.62
crystal system	monoclinic	orthorhombic	orthorhombic
space group	$P2_1/c$	*Pnma*	*Pnma*
a, Å	15.094(4)	16.779(5)	24.191(5)
b, Å	9.921(3)	14.807	13.926(3)
c, Å	18.717(4)	11.232(3)	8.5137(19)
α, deg	90.00	90.00	90.00
β, deg	97.921(8)	90.00	90.00
γ, deg	90.00	90.00	90.00
V, Å^3	2776.0(12)	2790.5(13)	2868.2(11)
ρ_{calc}, g cm^{-3}	1.640	1.691	4.385
temp, K	150	150	150
λ (Mo K_α), Å	0.71073	0.71073	0.71073
Z	4	4	4
$F(000)/\mu$ mm^{-1}	1404/1.057	1464/1.052	3288/27.648
$2\theta_{max}$ [deg]	36.42	46.24	30.50
reflns collected/unique	14 588/1962	21 422/2061	9692/649
R_{int}/GOF on F^2	0.1309/1.009	0.1051/0.903	0.1203/1.610
no. of parameters	372	209	224
R1[a](F_0), wR2[b](F_0) (all data)	0.0421, 0.1117	0.0430, 0.1190	0.0552, 0.1686
largest diff. peak, deepest hole, e Å^{-3}	0.277, −0.346	0.282, −0.249	1.072, −0.668

[a] $R = \sum||F_o| - |F_c||/\sum|F_o|$. [b] $wR = [\sum[w(F_o^2 - F_c^2)^2]/\sum(F_o^2)^2]^{1/2}$.

Scheme 1. Schematic Representation of the Protocol Followed for the Synthesis of Compounds 1−3

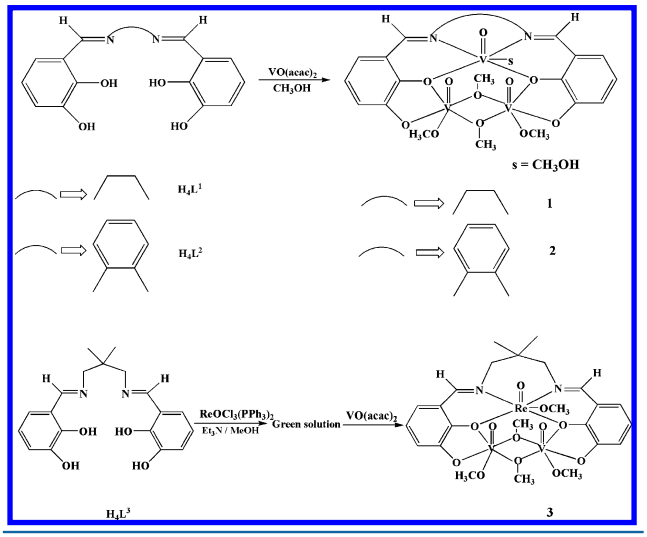

in this preparative procedure are the use of methanol as solvent and the exposures of the reaction media to atmospheric oxygen as confirmed by several control experiments. The upper compartment of these ligands has a Salen^{2-} type moiety that accommodates and stabilizes a VO^{2+} ion.[14] The remaining two vanadium centers are oxidized to VO^{3+} when exposed to atmospheric oxygen in methanol medium[4h] and are accommodated in the more flexible and spacious lower compartment of the ligands, thus providing trinuclear mixed-oxidation compounds with a rare type of V(V)−V(IV)−V(V) triangular core.[5c] The solvent CH_3OH plays a crucial role here as it supplies the $-OCH_3$ donor groups, both bridging and monodentate, to stabilize vanadium in the +5 oxidation state. No such compound has been isolated in our hand when the reactions were carried out with other alcohols like ethanol, 1-propanol, or 2-propanol as solvent.

The methodology has been extended to synthesize heterometal compounds with V(V)−Re(V)−V(V) combination following the same protocol, albeit with a minor modification, using the ligand, $[ReOCl_3(PPh_3)_2]$, and $[VO(acac)_2]$ in 1:1:2 mole ratio. Because Re(V) is much larger in size as compared to V(IV), a new ligand H_4L^3 with upper compartment of larger cavity size has been synthesized using 2,2-dimethyl-1,3-diaminopropane to provide enough flexibility in the ligand backbone to accommodate all three metal centers including Re(V). Compound $[L^3\{(Re^VO)(OCH_3)\}\{(V^VO)(OCH_3)(\mu\text{-}OCH_3)\}_2]$ **3** has composition similar to that of **1** and **2** with V(IV) being replaced by Re(V) in the upper compartment.

Compounds **1** and **2** are electrically neutral, and their charge neutralization requires that two of the vanadium centers are in +5 oxidation state while the third one is in +4 oxidation state. Because the alkoxido groups are known to stabilize vanadium in the +5 oxidation state,[4h] we believe the vanadium centers in the lower compartment are in the +5 state. In compound **3**, the upper compartment is occupied by Re(V) with an extra unit of positive charge as compared to **1** and **2**, neutralized by a methoxido group coordinated trans to its terminal oxido group. Of particular interest is the innocent behavior of the catecholate part of these ligands toward vanadium(v) in **1** and **2**. Because of their non-innocent nature, the $[V^V\text{-(catecholate}^{2-})]$ compounds[15] are also known to exist in their valence tautomeric $[V^{IV}\text{-(semiquinone)}^{1-}]$ form.[16]

All three compounds reported above have poor solubility characteristics. Both **1** and **2** are only sparingly soluble in dichloromethane, while **1** has a reasonable solubility in DMF. Compound **3**, on the other hand, is practically insoluble in all common organic solvents.

Selected IR data for the compounds (**1**−**3**) have been listed in the Experimental Section. Compound **1** displays two strong bands at 1639 cm^{-1} (corresponding band appears at 1608 and 1641 cm^{-1} in **2** and **3**, respectively) and 1589 cm^{-1}

dx.doi.org/10.1021/ic4013203 | Inorg. Chem. XXXX, XXX, XXX−XXX

(1579 and 1591 cm^{-1}) due to the ν(C═N) and ν(C═C) stretching modes of the coordinated Schiff-base and phenyl ring vibrations, respectively.[17] In addition, a sharp strong band is also observed at 1265 cm^{-1} (1265 and 1255 cm^{-1}) due to ν(C−O/phenolate) vibration.[17] The spectra of these compounds in the 1050−900 cm^{-1} range also reveal interesting information about their metal−oxygen vibrational modes. For compound **1**, a pair of strong bands at 1041 and 976 cm^{-1} are observed for the terminal ν(V═O_t) stretches, while for **2** only a single such mode in the form of a very strong band with distorted shape is observed at 991 cm^{-1}, apparently due to the overlap of two closely spaced ν(V═O_t) signals. This is as expected due to two types of vanadium centers [V(V) and V(IV)] present in **1**, while in **2** that difference is somewhat much less pronounced. Interestingly for compound **3**, two strong ν(M═O_t) bands are observed at 945 and 910 cm^{-1} as per our expectation.[18] The latter band is most likely due to ν(Re═O_t) vibrations due to the involvement of the heavier Re atom.[19]

Mass Spectrometry. ESI−MS spectra (in positive ion mode) for complexes **1** and **2** have been recorded in dichloromethane solution, and the data are listed in the Experimental Section. Both compounds demonstrate their respective molecular ion peaks due to the $[M - 2CH_3OH+Na]^+$ (for **1**) and $[M - CH_3OH + Na]^+$ (for **2**) ionic species. Unfortunately, the mass spectrum of **3** could not be recorded because of its lack of solubility in common organic solvent. In Figures 1 and 2 are displayed the isotope distribution patterns

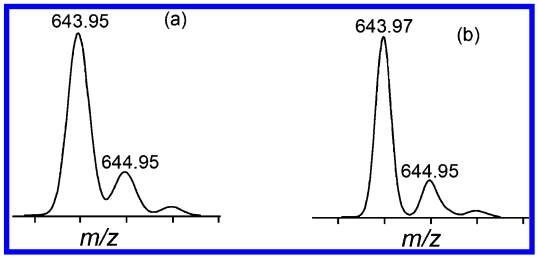

Figure 1. Molecular ion peak in the ESI mass spectrum (positive) for complex **1** in dichloromethane with (a) simulated and (b) observed isotopic distributions.

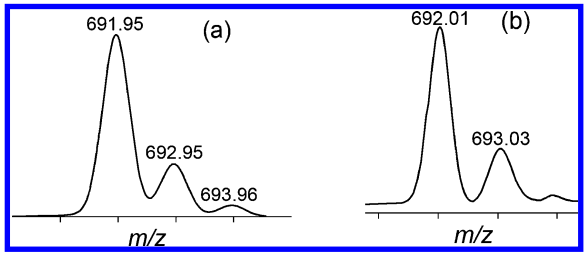

Figure 2. Molecular ion peak in the ESI mass spectrum (positive) for complex **2** in dichloromethane with (a) simulated and (b) observed isotopic distributions.

for the molecular ion peaks of **1** and **2**, respectively, along with their simulation patterns, thus providing support in favor of their proposed trinuclear compositions, which retain their integrity in CH_2Cl_2 solution.

Description of Crystal Structures. The molecular structures and the atom labeling schemes for compounds **1**−**3** are shown in Figures 3, 4, and 5, respectively, providing confirmatory evidence in support of their trinuclear compositions

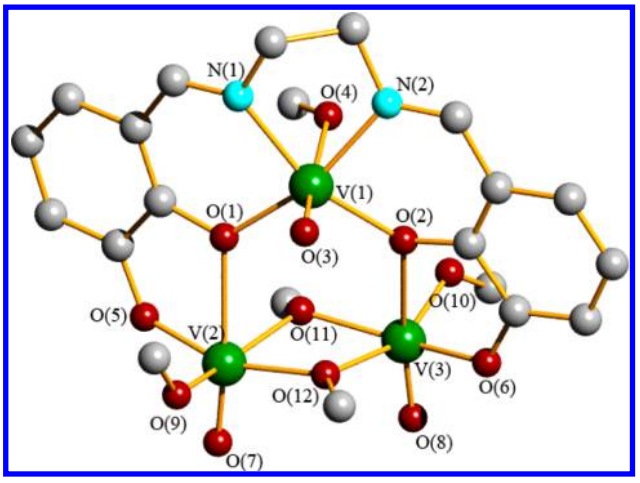

Figure 3. Molecular structure and the crystallographic numbering scheme for compound **1**. H atoms and solvent molecule have been omitted for clarity.

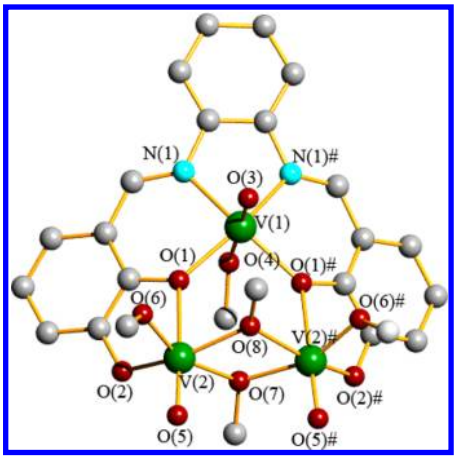

Figure 4. Molecular structure and atom labeling scheme for compound **2**. H atoms have been omitted for clarity.

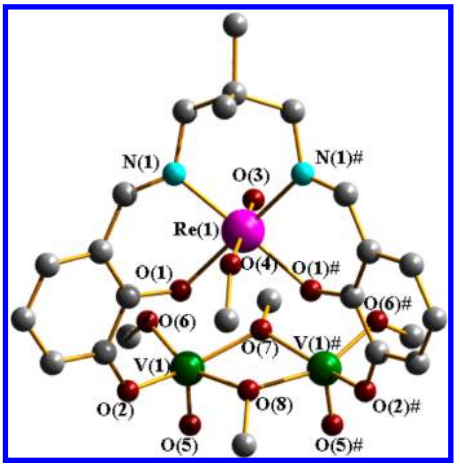

Figure 5. Molecular structure and atom labeling scheme for compound **3**. H atoms have been omitted for clarity.

with metal centers forming triangular cores. Their selected metrical parameters are listed in Tables 2 and 3. Compound **1** crystallizes in a monoclinic space group $P2_1/c$ with four molecular mass units accommodated per unit cell. Compounds **2** and **3**, on the other hand, crystallize in a more symmetric

dx.doi.org/10.1021/ic4013203 | Inorg. Chem. XXXX, XXX, XXX−XXX

Table 2. Selected Bond Lengths and Angles in 1 and 2

parameters	1	parameters	2
Bond Distances (Å)			
V1−O3	1.593(6)	V1−O3	1.587(5)
V1−O2	2.010(7)	V1−O1#	2.001(3)
V1−O1	2.025(7)	V1−O1	2.001(3)
V1−N2	2.060(9)	V1−N1#	2.077(4)
V1−N1	2.068(9)	V1−N1	2.077(4)
V1−O4	2.273(10)	V1−O4	2.379(6)
V2−O7	1.582(7)	V2−O5	1.595(3)
V2−O9	1.779(7)	V2−O6	1.804(3)
V2−O5	1.863(8)	V2−O2	1.855(3)
V2−O12	1.976(7)	V2−O8	1.977(3)
V2−O11	2.013(7)	V2−O7	2.008(3)
V2−O1	2.337(7)	V2−O1	2.312(3)
V3−O8	1.588(7)	V2#−O5#	1.595(3)
V3−O10	1.809(8)	V2#−O6#	1.804(3)
V3−O6	1.827(7)	V2#−O2#	1.855(3)
V3−O11	1.953(7)	V2#−O8	1.977(3)
V3−O12	1.993(6)	V2#−O7	2.008(3)
V3−O2	2.345(6)	V2#−O1#	2.312(3)
Bond Angles (deg)			
O3−V1−O2	98.2(3)	O3−V1−O1#	102.56(14)
O3−V1−O1	99.4(3)	O3−V1−O1	102.56(14)
O2−V1−O1	101.6(3)	O1#−V1−O1	96.47(18)
O3−V1−N2	98.3(3)	O3−V1−N1#	97.70(17)
O2−V1−N2	88.5(4)	O1#−V1−N1#	89.24(13)
O1−V1−N2	158.1(3)	O1−V1−N1#	157.16(14)
O3−V1−N1	96.0(3)	O3−V1−N1	97.70(17)
O2−V1−N1	162.0(4)	O1#−V1−N1	157.16(14)
O1−V1−N1	87.0(3)	O1−V1−N1	89.24(13)
N2−V1−N1	78.4(4)	N1#−V1−N1	77.6(2)
O3−V1−O4	176.0(4)	O3−V1−O4	175.2(3)
O2−V1−O4	85.8(4)	O1#−V1−O4	80.57(15)
O1−V1−O4	79.5(3)	O1−V1−O4	80.57(15)
N2−V1−O4	82.0(3)	N1#−V1−O4	78.58(18)
N1−V1−O4	80.2(4)	N1−V1−O4	78.58(18)
O7−V2−O9	101.4(3)	O5−V2−O6	100.40(18)
O7−V2−O5	94.2(4)	O5−V2−O2	97.89(17)
O9−V2−O5	98.2(3)	O6−V2−O2	98.28(16)
O7−V2−O12	98.2(3)	O5−V2−O8	102.31(19)
O9−V2−O12	92.3(3)	O6−V2−O8	89.41(16)
O5−V2−O12	161.8(3)	O2−V2−O8	156.72(16)
O7−V2−O11	100.8(3)	O5−V2−O7	95.34(18)
O9−V2−O11	154.1(3)	O6−V2−O7	158.03(17)
O5−V2−O11	93.3(3)	O2−V2−O7	94.61(15)
O12−V2−O11	71.4(3)	O8−V2−O7	72.22(15)
O7−V2−O1	169.2(3)	O5−V2−O1	173.32(17)
O9−V2−O1	84.1(3)	O6−V2−O1	83.86(13)
O5−V2−O1	75.7(3)	O2−V2−O1	76.31(12)
O12−V2−O1	90.8(3)	O8−V2−O1	82.77(15)
O11−V2−O1	76.4(2)	O7−V2−O1	81.99(15)
O8−V3−O10	98.3(4)	O5#−V2#−O6#	100.40(18)
O8−V3−O6	94.8(4)	O5#−V2#−O2#	97.89(17)
O10−V3−O6	100.2(3)	O6#−V2#−O2#	98.28(16)
O8−V3−O11	101.5(3)	O5#−V2#−O8	102.31(19)
O10−V3−O11	91.8(3)	O6#−V2#−O8	89.41(16)
O6−V3−O11	158.1(3)	O2#−V2#−O8	156.72(16)
O8−V3−O12	98.0(3)	O5#−V2#−O7	95.34(18)
O10−V3−O12	159.1(3)	O6#−V2#−O7	158.03(17)
O6−V3−O12	91.3(3)	O2#−V2#−O7	94.61(15)
O11−V3−O12	72.2(3)	O8−V2#−O7	72.22(15)
O8−V3−O2	168.9(3)	O5#−V2#−O1#	173.32(17)
O10−V3−O2	88.8(3)	O6#−V2#−O1#	83.86(13)
O6−V3−O2	75.5(3)	O2#−V2#−O1#	76.31(12)
O11−V3−O2	86.7(3)	O8−V2#−O1#	82.77(15)
O12−V3−O2	77.2(2)	O7−V2#−O1#	81.99(15)

orthorhombic space group *Pnma* with as many molecular mass units accommodated per cell. Thus, unlike in **1**, compound **2** has a 2-fold symmetry that renders the two vanadium centers V(2) and V(2)# in the lower ligand compartment exactly identical. The V(1) centers in the upper compartment of both compounds have distorted octahedral environments. Four donor atoms O(1), N(1), N(2), O(2) [O(1), N(1), N(1)#, O(1)# in **2**] from the Salen-type moiety of this compartment occupy the basal plane. The apical positions are taken up by the terminal oxido atom O(3) and the oxygen atom of the coordinated methanol molecule O(4). The trans angles O(1)−V(1)−N(2) 158.1(3)° [O(1)−V(1)−N(1)# 157.16(14)°] and O(2)−V(1)−N(1) 162.0(4)° [N(1)−V(1)−O(1)# 157.16(14)°] are somewhat compressed, forcing the V(1) atom to move out of the basal plane by 0.286 Å [0.365 Å] toward the apical oxido atom O(3). In the lower compartment, both the vanadium centers V(2) and V(3) [V(2) and V(2)#] also have octahedral environments, each made up of an O_6 core, which differ marginally in **1** and are identical in **2**. The basal positions around V(2) in **1** are completed by O(5), O(9), O(12), O(11) donor atoms [O(6), O(2), O(7), O(8) in **2**], three of which (two bridging and a monodentate) are contributed by the methoxido donor atoms, which stabilize the metal center in the +5 oxidation state.[4h] The apical positions, on the other hand, are occupied by the terminal oxido atom O(7) [O(5)] and a bridging phenoxido atom O(1). The coordination environment around V(3) [V(2)#] is almost [exactly] identical to that of V(2). The terminal V=O_t distances V(1)−O(3) 1.593(6), V(2)−O(7) 1.582(7), and V(3)−O(8) 1.588(7) Å [1.587(5), 1.595(3), and 1.595(3) Å, respectively] are all in the expected range. The V(1)−O(4) distance 2.273(10) Å [2.379(6) Å] is much elongated due to trans labilization influence of the terminal oxido group. The V(2)−O(9) 1.779(7), V(2)−O(11) 2.013(7), and V(2)−O(12) 1.976(7) Å distances [corresponding distances in **2** are V(2)−O(6) 1.804(3), V(2)−O(7) 2.008(3), and V(2)−O(8) 1.977(3) Å] are in the expected ranges for terminal and bridging methoxido groups, respectively.[5e,20] The trans angles in the basal plane O(5)−V(2)−O(12) 161.8(3)° [158.03(17)°] and O(9)−V(2)−O(11) 154.1(3)° [156.72(16)°] are much short of linearity, forcing the V(2) atom to move out of the basal plane by 0.261 Å [0.296 Å] toward the terminal oxido atom O(7) [O(5)] and generate distorted octahedral geometry around the metal center. For V(3) atom, the trans angles O(10)−V(3)−O(12) and O(6)−V(3)−O(11) are 159.1(3)° and 158.1(3)°, respectively, and the V(3) atom is displaced from the mean basal plane by 0.280 Å [0.296 Å]. The dihedral angle between the two basal planes containing V(1) and V(2) is 87.32° and V(1) and V(3) is 87.77° [both are 80.72° in **2**]. The distances between the V(1)···V(2) and V(1)····V(3) centers are 3.880 and 3.915 Å,

dx.doi.org/10.1021/ic4013203 | *Inorg. Chem.* XXXX, XXX, XXX−XXX

Table 3. Relevant Bond Distances and Angles in 3

Bond Distances (Å)			
Re1−O3	1.72(2)	V1−O2	1.869(17)
Re1−O4	1.97(2)	V1−O7	1.974(16)
Re1−O1	2.071(15)	V1−O8	1.999(16)
Re1−O1#	2.071(15)	V1#−O5#	1.52(2)
Re1−N1	2.09(2)	V1#−O6#	1.80(2)
Re1−N1#	2.09(2)	V1#−O2#	1.869(17)
V1−O5	1.52(2)	V1#−O7	1.974(16)
V1−O6	1.80(2)	V1#−O8	1.999(16)
Bond Angles (deg)			
O3−Re1−O4	178.3(9)	O6−V1−O8	156.9(10)
O3−Re1−O1	95.6(6)	O2−V1−O8	91.2(8)
O4−Re1−O1	85.6(5)	O7−V1−O8	72.1(9)
O3−Re1−O1#	95.6(6)	O5−V1−O1	172.2(8)
O4−Re1−O1#	85.6(5)	O2−V1−O1	76.3(7)
O1−Re1−O1#	93.9(8)	O7−V1−O1	83.2(8)
O3−Re1−N1	92.3(7)	O8−V1−O1	79.2(7)
O4−Re1−N1	86.5(6)	V1−O7−V1#	106.9(12)
O1−Re1−N1	87.1(8)	O5#−V1#−O6#	101.7(10)
O1#−Re1−N1	172.0(7)	O5#−V1#−O2#	97.4(9)
O3−Re1−N1#	92.3(7)	O6#−V1#−O2#	100.2(8)
O4−Re1−N1#	86.5(6)	O5#−V1#−O7	101.9(9)
O1−Re1−N1#	172.0(7)	O6#−V1#−O7	91.(1)
O1#−Re1−N1#	87.1(8)	O2#−V1#−O7	90.3(8)
N1−Re1−N1#	90.7(12)	O5#−V1#−O8	96.6(10)
O5−V1−O6	101.7(10)	O6#−V1#−O8	156.9(10)
O5−V1−O2	97.4(9)	O2#−V1#−O8	91.2(8)
O6−V1−O2	100.2(8)	O7−V1#−O8	72.1(9)
O5−V1−O7	101.9(9)	O5#−V1#−O1#	172.2(8)
O6−V1−O7	90.3(8)	O2#−V1#−O1#	76.3(7)
O2−V1−O7	155.7(9)	O7−V1#−O1#	83.2(8)
O5−V1−O8	96.6(10)	O8−V1#−O1#	79.2(7)

respectively [3.883 Å]. The V(2)···V(3) distance is 3.191 Å [3.196 Å].

Interestingly, both compounds **1** and **2** are trapped valence (class I)[21] mixed-oxidation compounds with the V(1) center being in the +4 oxidation state with larger ionic radius as compared to V(2) and V(3) [V(2#)] sites, which are in the +5 oxidation state as reflected from the bond length data. Thus, in **1**, the V(1)−N(1) distance 2.068(9) Å is much larger as compared to the V(2)−O(5) distance 1.863(8) Å. On that basis, the bridging V(1)−O(1) distance 2.025(7) Å should have been larger than the V(2)−O(1) distance. Interestingly, contrary to that expectation, the later distance 2.337(7) Å is much larger due to the opposing effect of the strong trans labilization influence of the terminal V(2)−O(7) bond. Because the bridging V(2)−O(1)−V(1) angle 127.5(4)° is much short of linearity, it restricts the symmetry constrained d_{xy} orbital of V(1) center that accommodates the unpaired electron, to interact effectively with the remaining vanadium centers, thus generating a trapped valence system in this case.[3b]

The molecular structure of the remaining compound $[L^3\{(Re^VO)(OCH_3)\}\{(V^VO)(OCH_3)(\mu\text{-}OCH_3)\}_2]$ **3** is quite similar to those of **1** and **2**, the only difference being in the upper compartment where V(IV) in the latter two compounds is replaced by a Re(V) center. The necessary charge balance requires a concomitant replacement of the coordinated methanol O(4) in **2** by a methoxy group in **3** as evident from the short Re(1)−O(4) bond length of 1.95(3) Å as compared to the larger V(1)−O(4) distance of 2.379(6) Å. The coordination environments around the vanadium centers are very much the same as observed in **2**. The Re(1)−O(3) 1.716(19) Å and Re(1)−O(4) 1.95(3) Å bonds are as expected for $Re^V{=}O_t$ and Re^V−alkoxide distances, respectively.[22] The V(1)−O(5) distance 1.54(2) Å is as expected for the terminal $V{=}O_t$ bond. Also, the V(1)−O(6), V(1)−O(7), and V(1)−O(8) distances of 1.78(3), 1.95(2), and 1.98(2) Å, respectively, are in the expected ranges for terminal and bridging $-OCH_3$ distances in a vanadium(V) compound.[5e,20] The trans angles O(1)−Re(1)−N(1)# and O(1)#-Re(1)−N(1) 170.6(12)° are slightly short of linearity, which forces the Re(1) atom to move out of the basal plane by 0.164 Å toward the apical oxido atom O(3). The V(1) atom, on the other hand, is displaced by 0.306 Å [same for V(1)# atom] from its basal plane containing O(2), O(6), O(7), and O(8) atoms. The Re···V distance is 3.995 Å, and that between the two V centers is 3.163 Å. The dihedral angle between the basal planes containing the Re and V atom is 76.02°.

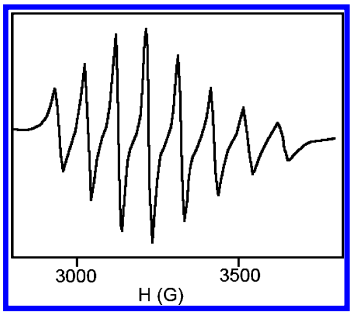

Figure 6. X-band EPR spectrum of compound **1** at room temperature in DMF.

EPR Spectroscopy. The EPR spectrum of compound **1** has been recorded in DMF (Figure 6) at ambient temperature. Unfortunately, the data are not available for compound **2** because of its poor solubility in common organic solvents. The spectrum shows an 8-line profile (for ^{51}V, $I = 7/2$) with $\langle g \rangle = 1.972$ and $\langle A \rangle = 86.61 \times 10^{-4}$ cm^{-1}, providing indication of a valence-trapped situation for the odd electron of this V(V)−V(IV)−V(V) core on the time-scale of EPR spectroscopy. Had the unpaired electron been delocalized on all three vanadium centers, one would have expected a 22-line spectrum or a 15-line one if the delocalization covered two of the vanadium centers.[4a,c,h,i] Indirect support in favor of such a trapped-valence character also comes from the results of X-ray crystallography, which reveals the V(1) center to be in the +4 oxidation state and V(2) and V(3) in the +5 state. Similar trapped-valence character has been also reported for the only other triangular V(V)−V(IV)−V(V) mixed-oxidation compound reported thus far in the literature.[5c] Compound **1** thus retains its structural integrity in DMF solution.

X-ray Photoelectron Spectroscopy. The XPS analysis of compound **1** also provides convincing evidence in support of a trapped-valence mixed-oxidation V(V)−V(IV)−V(V) composition. The spectral profile depicted in Figure 7 contains two well-resolved peaks at 515.14 and 522.14 eV, which correspond to the binding energy of the vanadium $2p_{3/2}$ and $2p_{1/2}$ electrons in the oxidation states +5 and +4, respectively.[23] A similar result from XPS study has been reported earlier for a mixed-oxidation divanadium [V(IV/V)] compound.[4m]

dx.doi.org/10.1021/ic4013203 | Inorg. Chem. XXXX, XXX, XXX−XXX

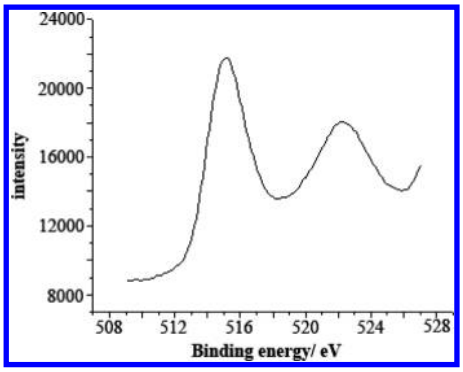

Figure 7. High-resolution XPS spectrum of vanadium (2p) in compound **1**.

Electronic Spectroscopy. The electronic spectrum of **1** in DMF in the visible−NIR range (200−1200 nm) is displayed in Figure 8, which features no band in the NIR region, thus

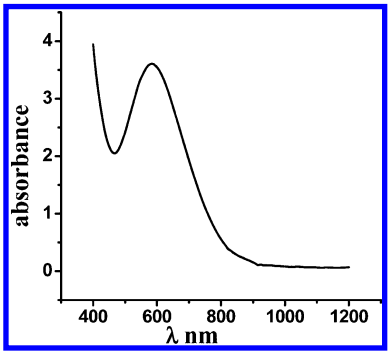

Figure 8. Electronic absorption spectrum of **1** in DMF (concentration: 1×10^{-3} M).

confirming its status as a typical trapped-valence compound[21] in solution as established already by EPR spectroscopy. A strong band at λ_{max} = 583 nm (ε = 3600 $M^{-1}\,cm^{-1}$), possibly originating from a $PhO^{-}\rightarrow V$ charge transfer,[4e,24] is the only feature observed in the visible region that masks the d−d bands expected to be seen in this region due to a vanadyl center.[4k,25] Unfortunately, because of solubility restrictions, the spectra of **2** and **3** remain unreported.

Electrochemistry. The cyclic voltammogram of **1** has been recorded at a glassy carbon working electrode under an atmosphere of purified dinitrogen in DMF solution (0.1 M TBAP) at 25 °C in the potential range from −0.1 to +1.1 V vs Ag/AgCl reference. The voltammogram (Figure 9) displays a

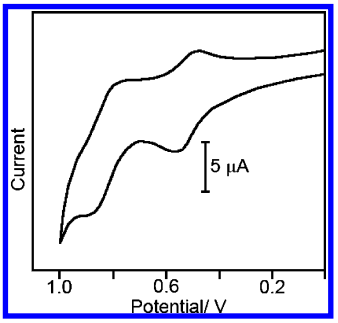

Figure 9. Cyclic voltammogram of compound **1** in DMF; potentials vs Ag/AgCl, 0.1 M TBAP at a glassy carbon working electrode, scan rate of 100 mV s^{-1}.

couple of redox processes in the positive potential range, which includes a reversible electron transfer at $E_{1/2}$ = 0.52 V (ΔE_p = 80 mV), tentatively arising from a metal-based [V(IV/V)] oxidation as represented by eq 1. The remaining oxidation observed at a higher anodic potential $E_{1/2}$ = 0.83 V (ΔE_p = 100 mV) is most certainly originating from a ligand-based oxidation involving one of the catecholate moieties. The cathodic part of the later process reveals a decrease in current height, thus confirming the onset of a ligand decomposition process after the initial oxidation. Under identical experimental conditions, the ferrocenium/ferrocene couple appears at 0.60 V (ΔE_p = 90 mV). Coulometric confirmations of electron stoichiometry for these processes have been vitiated by the instability of this compound in the longer time-scale of CPC experiment.

$$[L^1(V^{IV}O)(V^{V}O)_2(OCH_3)_4] \underset{E_{1/2}=0.52V}{\overset{-e^-}{\rightleftharpoons}} [L^1(V^{V}O)_3(OCH_3)_4]^+ \quad (1)$$

The voltammetry experiments with compounds **2** and **3** remain unreported due to their poor solubility in common organic solvents.

Bond Valence Sum Calculation. The use of bond valence sum (BVS) calculation[26] provides further support in favor of a V(V)−V(IV)−V(V) valence distribution in the trinuclear compounds **1** and **2**. In short, the bond valence (s_{ij}) and the bond length (r_{ij}) between two atoms (i, j) are related by eq 2 where r_0 and B are two empirically determined parameters, the former being the characteristic of the bond in question.[26] For a polyatomic system containing a central metal atom, the bond valence s_{ij} of a particular bond may be contemplated as the amount of electrons by which the metal center (i) is depleted in forming that bond with ligand (j). Consequently, the BVS (V_i) of the metal atom is a measure of the total number of electrons it loses (i.e., oxidation state) in forming that compound and is calculated using eq 3. It appears from eq 2 that the s_{ij} contribution of a particular bond decreases as the length (r_{ij}) of that bond increases and vice versa. Recently, BVS model has been successfully applied to estimate the vanadium oxidation states in native as well as reduced bromoperoxidase.[27] This method worked really well when applied also to many model compounds with vanadium in IV and V oxidation states.[27] In our calculation, we have used the required r_0 values available from the literature,[27,28] and B, the empirical constant, is taken as 0.37. The r_{ij} values are taken as the bond lengths of the individual bonds determined by X-ray crystallography. In Table 4 are summarized the BVS values calculated for the individual vanadium centers in **2** taken as a representative compound. Similar results are also obtained for compound **1** (Table S1 in the Supporting Information). In this calculation, all of the vanadium centers have been considered either in +4 or in +5 oxidation states. The results have convincingly established the V(1) center to be in the +4 oxidation state, and the rest of the vanadium centers are in the +5 state.

$$s_{ij} = \exp[(r_0 - r_{ij})/B] \quad (2)$$

$$V_i = \sum_j s_{ij} \quad (3)$$

bond	r_0, Å
V^{4+}−O	1.784
V^{5+}−O	1.803
V^{4+}−N	1.874
V^{5+}−N	1.894

dx.doi.org/10.1021/ic4013203 | Inorg. Chem. XXXX, XXX, XXX−XXX

Table 4. Bond Valence Sum Calculated for the Vanadium Centers in 2

vanadium	bond description	r_0, Å (considering V(IV))	r_0, Å (considering V(V))	r_{ij}, Å	s_{ij} (considering V(IV))	s_{ij} (considering V(V))	$V_{ij} = \sum_j s_{ij}$ (considering V(IV))	$V_{ij} = \sum_j s_{ij}$ (considering V(V))
V(1)	V1−O3	1.784	1.803	1.587	1.70	1.79	4.14	4.36
	V1−O1#			2.001	0.55	0.58		
	V1−O1			2.001	0.55	0.58		
	V1−O4			2.379	0.20	0.21		
	V1−N1#	1.874	1.894	2.077	0.57	0.60		
	V1−N1			2.077	0.57	0.60		
V(2)	V2−O5	1.784	1.803	1.595	1.66	1.75	4.79	5.03
	V2−O6			1.804	0.94	0.99		
	V2−O2			1.855	0.82	0.86		
	V2−O8			1.977	0.59	0.62		
	V2−O7			2.008	0.54	0.56		
	V2−O1			2.312	0.24	0.25		
V(2)#	V2#−O5#	1.784	1.803	1.595	1.66	1.78	4.79	5.03
	V2#−O6#			1.804	0.94	0.98		
	V2#−O2#			1.855	0.82	0.93		
	V2#−O8			1.977	0.59	0.66		
	V2#−O7			2.008	0.54	0.59		
	V2#−O1#			2.312	0.24	0.23		

CONCLUSIONS

Mixed-oxidation trinuclear vanadium compounds **1** and **2** in V(V)−V(IV)−V(V) valence distribution have been synthesized and characterized in the solid state by single-crystal X-ray diffraction analysis. For **1**, results of both EPR and XPS spectroscopy have confirmed this mixed-valence compound to be of trapped-valence type. Bond valence sum calculation also supported this view. Replacement of the V(IV) center in these compounds by Re(V) has led us to the successful isolation of a heterotrinuclear compound (**3**) with a V(V)−Re(V)−V(V) core. Result of X-ray structure analysis has confirmed the details of the molecular structure of this interesting heterotrinuclear compound with all oxido−metal ions forming a triangular core.

ASSOCIATED CONTENT

Supporting Information

BVS data for compound **1** (Table S1), and X-ray crystallographic files in CIF format for compounds **1**−**3**. This material is available free of charge via the Internet at http://pubs.acs.org.

AUTHOR INFORMATION

Corresponding Author

*E-mail: icmc@iacs.res.in.

Notes

The authors declare no competing financial interest.

ACKNOWLEDGMENTS

This work was supported by the Council of Scientific and Industrial Research (CSIR), New Delhi. K.B., M.M., S.M.T.A., and M.C.M. also thank the CSIR for the award of Research Fellowships. The single-crystal X-ray diffraction data were recorded on an instrument supported by DST, New Delhi as a National facility at IACS under the IRHPA program. XPS facility was also provided by DST through the Unit of Nanoscience at IACS.

REFERENCES

(1) See, for example: (a) Rehder, D. *Bioinorganic Vanadium Chemistry*; Wiley: Chichester, UK, 2008. (b) Kustin, K., Pesssoa, J. C., Crans, D. C., Eds. *Vanadium: The Versatile Metal*; ACS Symposium Series 974; American Chemical Society: Washington, DC, 2007. (c) Tracey, A. S.; Willsky, G. R.; Takeuchi, E. S. *Vanadium Chemistry, Biochemistry, Pharmacology and Practical Applications*; CRC Press: Boca Raton, FL, 2007. (d) Crans, D. C.; Smee, J. J.; Gaidamauskas, E.; Yang, L. *Chem. Rev.* **2004**, *104*, 849. (e) Fraústo da Silva, J. J. R.; Williams, R. J. P. *The Biological Chemistry of the Element*; Oxford University Press: Oxford, UK, 2001. (f) Rehder, D. *Coord. Chem. Rev.* **1999**, *182*, 297. (g) Müller, A.; Peters, F.; Pope, M. T.; Gatteschi, D. *Chem. Rev.* **1998**, *98*, 849. (h) Sigel, H., Sigel, A., Eds. *Metal Ions in Biological Systems*; Marcel Dekker: New York, 1995; Vol. *31*. (i) Rehder, D. *Angew. Chem., Int. Ed. Engl.* **1991**, *30*, 148.

(2) See, for example: (a) Hamstra, B. J.; Houseman, A. L. P.; Colpas, G. J.; Kampf, J. W.; LoBrutto, R.; Frasch, W. D.; Pecoraro, V. L. *Inorg. Chem.* **1997**, *36*, 4866. (b) Keramidas, A. D.; Miller, S. N.; Anderson, O. P.; Crans, D. C. *J. Am. Chem. Soc.* **1997**, *119*, 8901. (c) Holwerda, R. A.; Whittlesey, B. R.; Nilges, M. J. *Inorg. Chem.* **1998**, *37*, 64. (d) Dutta, S. K.; Samanta, S.; Kumar, S. B.; Han, O. H.; Burckel, P.; Pinkerton, A. A.; Chaudhury, M. *Inorg. Chem.* **1999**, *38*, 1982.

(3) (a) Boas, L. V.; Pessoa, J. C. *Comprehensive Coordination Chemistry*; Pergamon: Oxford, 1987; Vol. 3, pp 453−583. (b) Young, C. G. *Coord. Chem. Rev.* **1989**, *96*, 89.

(4) (a) Nishizawa, M.; Hirotsu, K.; Ooi, S.; Saito, K. *J. Chem. Soc., Chem. Commun.* **1979**, 707. (b) Kojima, A.; Okazaki, K.; Ooi, S.; Saito, K. *Inorg. Chem.* **1983**, *22*, 1168. (c) Launay, J.-P.; Jeannin, Y.; Daoudi, M. *Inorg. Chem.* **1985**, *24*, 1052. (d) Costa-Pessoa, J.; Silva, J. A. L.; Vieira, A. L.; Vilas-Boas, L.; OBrien, P. O.; Thornton, P. *J. Chem. Soc., Dalton Trans.* **1992**, 1745. (e) Schulz, D.; Weyhermüller, T.; Wieghardt, K.; Nuber, B. *Inorg. Chim. Acta* **1995**, *240*, 217. (f) Fukuda, I.; Matsushima, H.; Maeda, K.; Koikawa, M.; Tokii, T. *Chem. Lett.* **1997**, 463. (g) Copeland, E. P.; Kahwa, I. A.; Mague, J.; McPherson, G. L. *J. Chem. Soc., Dalton Trans.* **1997**, 2849. (h) Dutta, S. K.; Kumar, S. B.; Bhattacharyya, S.; Tiekink, E. R. T.; Chaudhury, M. *Inorg. Chem.* **1997**, *36*, 4954. (i) Mondal, S.; Ghosh, P.; Chakravorty, A. *Inorg. Chem.* **1997**, *36*, 59. (j) Mahroof-Tahir, M.; Keramidas, A. D.; Goldfarb, R. B.; Anderson, O. P.; Miller, M. M.; Crans, D. C. *Inorg. Chem.* **1997**, *36*, 1657. (k) Ghosh, S.; Nanda, K. K.; Addison, A. W.; Butcher, R. J. *Inorg. Chem.* **2002**, *41*, 2243. (l) Wang, D.; Behrens, A.; Farahbakhsh, M.; Gatjens, J.; Rehder, D. *Chem.-Eur. J.* **2003**, *9*, 1805. (m) Chen, C.-Y.; Zhou, Z.-H.; Chen, H.-B.; Huang, P.-Q.; Tsai, K.-R.; Chow, Y. L. *Inorg. Chem.* **2008**, *47*, 8714.

(5) (a) Bino, A.; Cohen, S.; Heitner-Wirguin, C. *Inorg. Chem.* **1982**, *21*, 429. (b) Müller, A.; Krickerneyer, E.; Penk, M.; Walberg, H.-J.; Bogge, H. *Angew. Chem., Int. Ed. Engl.* **1987**, *26*, 1045. (c) Codd, R.; Hambley, T. W.; Lay, P. A. *Inorg. Chem.* **1995**, *34*, 877. (d) Jin, Y.; Lee,

dx.doi.org/10.1021/ic4013203 | *Inorg. Chem.* XXXX, XXX, XXX−XXX

H.-I.; Pyo, M.; Lah, M. S. *Dalton Trans.* **2005**, 797. (e) Sutradhar, M.; Kirillova, M. V.; da Silva, M. F. C. G.; Martins, L. M. D. R. S.; Pombeiro, A. J. L. *Inorg. Chem.* **2012**, *51*, 11229.
(6) Rowe, R. A.; Jones, M. M. *Inorg. Synth.* **1957**, *5*, 113.
(7) Chatt, J.; Rowe, G. A. *J. Chem. Soc.* **1962**, 4019.
(8) Perrin, D. D.; Armarego, W. L. F.; Perrin, D. R. *Purification of Laboratory Chemicals*, 2nd ed.; Pergamon: Oxford, UK, 1980.
(9) Sheldrick, G. M. *SADABS, Program for Empirical Absorption Correction of Area Detector Data*; University of Göttingen: Göttingen, Germany, 1996.
(10) Sheldrick, G. M. *Acta Crystallogr.* **1990**, *46A*, 467.
(11) Sheldrick, G. M. *SHELXL-97, Program for Crystal Structure Refinements*; University of Göttingen: Göttingen, Germany, 1996.
(12) *SAINT-plus, Software Users' Guide, Version 6.0*; Bruker Analytical X-ray Systems: Madison, WI, 1999.
(13) *DIAMOND, Visual Crystal Structure Information System, version 3.1*; Crystal Impact: Bonn, Germany, 2004.
(14) Pfeiffer, P.; Breith, E.; Lülle, E.; Tsumaki, T. *Justus Liebigs Ann. Chem.* **1933**, *503*, 84.
(15) Pooransingh, N.; Pomerantseva, E.; Ebel, M.; Jantzen, S.; Rehder, D.; Polenova, T. *Inorg. Chem.* **2003**, *42*, 1256.
(16) Chatterjee, P. B.; Bhattacharya, K.; Kundu, N.; Choi, K.-Y.; Clérac, R.; Chaudhury, M. *Inorg. Chem.* **2009**, *48*, 804.
(17) Fairhurst, S. A.; Hughes, D. L.; Leigh, G. J.; Sanders, J. R.; Weisner, J. *J. Chem. Soc., Dalton Trans.* **1994**, 2591.
(18) Nugent, W. A.; Mayer, J. M. *Metal-Ligand Multiple Bonds: The Chemistry of Transition Metal Complexes Containing Oxo, Nitrido, Imido, Alkylidene, or Alkylidyne Ligands*; John Wiley & Sons: New York, 1988.
(19) Middleton, A. R.; Masters, A. F.; Wilkinson, G. *J. Chem. Soc., Dalton Trans.* **1979**, 542.
(20) (a) Caughlan, C. N.; Smith, H. M.; Watenpaugh, K. *Inorg. Chem.* **1966**, *5*, 2131. (b) Hillerns, F.; Olbrich, F.; Behrens, U.; Rehder, D. *Angew. Chem., Int. Ed. Engl.* **1992**, *31*, 447. (c) Crans, D. C.; Felty, R.; Miller, M. M. *J. Am. Chem. Soc.* **1991**, *113*, 265.
(21) (a) Robin, M. B.; Day, P. *Adv. Inorg. Radiochem.* **1967**, *10*, 247. (b) Hush, N. S. *Prog. Inorg. Chem.* **1967**, *8*, 391.
(22) van Bommel, K. J. C.; Verboom, W.; Kooijman, H.; Spek, A. L.; Reinhoudt, D. N. *Inorg. Chem.* **1998**, *37*, 4197.
(23) Silversmit, G.; Depla, D.; Poelman, H.; Marin, G. B.; De Gryse, R. *J. Electron Spectrosc. Relat. Phenom.* **1991**, *57*, 189.
(24) Bonadies, J. A.; Carrano, C. J. *J. Am. Chem. Soc.* **1986**, *108*, 4088.
(25) Selbin, J. *Coord. Chem. Rev.* **1966**, *1*, 293.
(26) (a) Brown, I. D. *Chem. Soc. Rev.* **1978**, *7*, 359. (b) Brown, I. D. *Acta Crystallogr., Sect. B* **1992**, *48*, 553.
(27) Carrano, C. J.; Mohan, M.; Holmes, S. M.; de la Rosa, R.; Butler, A.; Charnock, J. M.; Garner, C. D. *Inorg. Chem.* **1994**, *33*, 646.
(28) Brown, I. D.; Altermatt, D. *Acta Crystallogr., Sect. B* **1985**, *41*, 244.

dx.doi.org/10.1021/ic4013203 | *Inorg. Chem.* XXXX, XXX, XXX−XXX